

Figure S1. Deleting snapin in mouse brains impairs recruitment of dynein DIC to LE membranes. (A and B) Immunoprecipitation (A) and quantitative analysis (B) showing reduced association of DIC with LEs in *snapin* flox/flox cKO mouse brains. LEs were immunoprecipitated from light membrane fractions of adult mouse brains with superparamagnetic beads coated with an anti-Rab7 antibody or normal IgG as a control. Bead-bound membrane organelles were resolved by PAGE and sequentially detected with antibodies on the same membranes after stripping between applications of each antibody. Note that reduced tethering of dynein DIC to LEs in *snapin* flox/flox cKO mice (A, red box) is specific because LE markers Rab7 and LAMP-2 were equally associated with the organelles in WT and *snapin* cKO mouse brains. Data were analyzed from three pairs ($n = 3$) of mice, normalized by integrated protein intensity from WT mice, and expressed as means \pm SEM. Input: 10% of total proteins in immunoprecipitation. (C) Snapin–dynein motor complexes were coimmunoprecipitated by an anti-snapin antibody from brain homogenates. Snapin-associated proteins were sequentially detected on the same membranes with antibodies against dynein motor subunits DHC, DIC, and dynactin p150^{Glued}. Input: 10% of brain homogenates in coimmunoprecipitation. (D and E) Representative kymographs (D) and quantitative analysis (E) showing relative mitochondrial motility in DRG neurons expressing HA-snapin-L99K or HA control. Total number of neurons examined is 17 for each transfection condition. Error bars: SEM. Mann–Whitney test. Bars, 10 μ m.

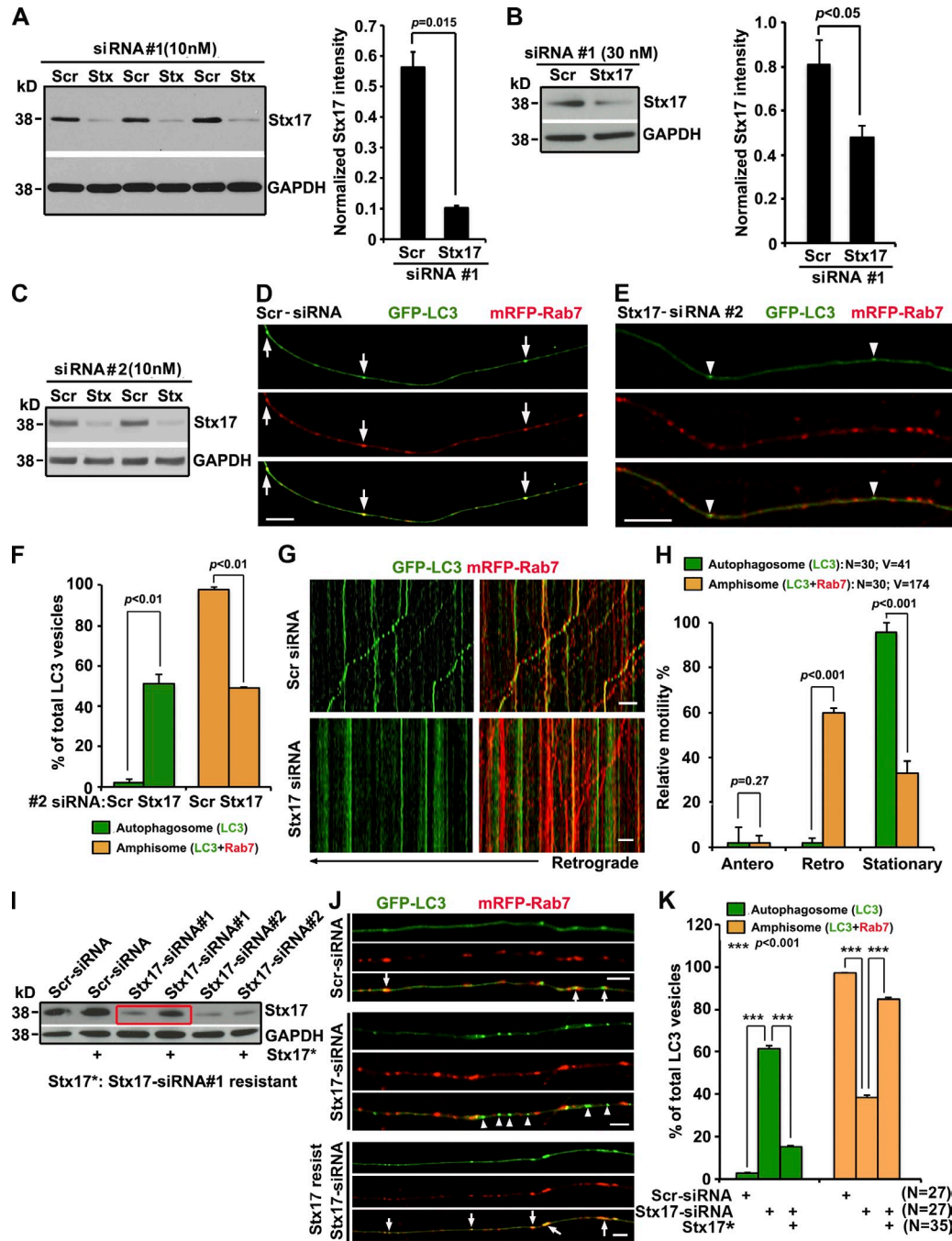


Figure S2. **Depleting Stx17 blocks formation of amphisomes and immobilizes AVs along axons.** (A) Effective knockdown of endogenous Stx17 with Stx17-siRNA #1 in HEK293T cells. Cells were transfected with 10 nM Scr- or Stx17-siRNA #1 oligonucleotides and analyzed by immunoblotting 3 d after transfection using antibodies against Stx17 and GAPDH. The mean intensity of Stx17 was normalized to GAPDH from the same blots and expressed as a ratio relative to control Scr-siRNA. Data were collected from three repeats ($n = 3$). (B) Effective knockdown of Stx17 with Stx17-siRNA #1 in DRG neurons. Neurons were transfected at DIV0 with 30 nM Scr- or Stx17-siRNA #1 oligonucleotides and analyzed by immunoblotting 3 d after transfection using antibodies against Stx17 and GAPDH. Data were collected from three repeats ($n = 3$). Note that the remaining Stx17 signals could be a result of (a) siRNA suppression but not fully depletion of endogenous Stx17 or (b) limited transfection efficiency in DRG neurons. Only transfected neurons were selected for imaging analysis. (C) Effective knockdown of endogenous Stx17 with Stx17-siRNA#2 in HEK293T cells. Cells were transfected with 10 nM Scr- or Stx17-siRNA#2 oligonucleotides and analyzed by immunoblotting 3 d after transfection using antibodies against Stx17 and GAPDH. (D–F) Representative images of DRG neuron axons (D and E) and quantitative analysis (F) showing that depleting Stx17 with Stx17-siRNA#2 blocks formation of amphisomes. DRG neurons were cotransfected with GFP-LC3, mRFP-Rab7, and Scr-siRNA or Stx17-siRNA#2 (30 nM) at DIV0 and subjected to live imaging at DIV3 after a 3-h starvation. Imaging was performed on axonal segments between middle to distal regions. Arrows indicate amphisomes colabeled with LC3 and Rab7 (D), whereas arrowheads indicate autophagosomes not labeled with Rab7 (E). (F) Note a robust increase in the number of autophagosomes and decrease in amphisomes in neurons expressing Stx17-siRNA#2. Number of vesicles was expressed as a percentage of the total number of LC3-labeled organelles. Data were quantified from 30 axons and the total number of 215 AVs in greater than three experiments. (G and H) Representative kymographs (G) and quantitative analysis (H) showing that amphisomes display predominant retrograde motility, whereas depleting Stx17 immobilizes autophagosomes during 1.5-min dual-channel time-lapse imaging. Data were quantified from number of AVs (V) in the total number of neurons (N) from greater than three experiments. (I–K) The siRNA#1-resistant Stx17 silent mutant (Stx17*) rescues the knockdown phenotypes. Stx17* was created by substituting three nucleotides in the Stx17-siRNA#1-targeting region (A528G, G531A, and C534T). Stx17* expression was resistant to Stx17-siRNA#1 interference (I, red box) and abolished the inhibitory role of Stx17 knockdown in amphisomal formation in DRG neurons (J and K). Arrows indicate amphisomes colabeled with LC3 and Rab7, whereas arrowheads indicate autophagosomes not labeled by Rab7. Data were quantified from the total number of neurons (N) from more than three experiments. Error bars: SEM. Student's t test. Bars: (D, E, and J) 5 μ m; (G) 10 μ m.

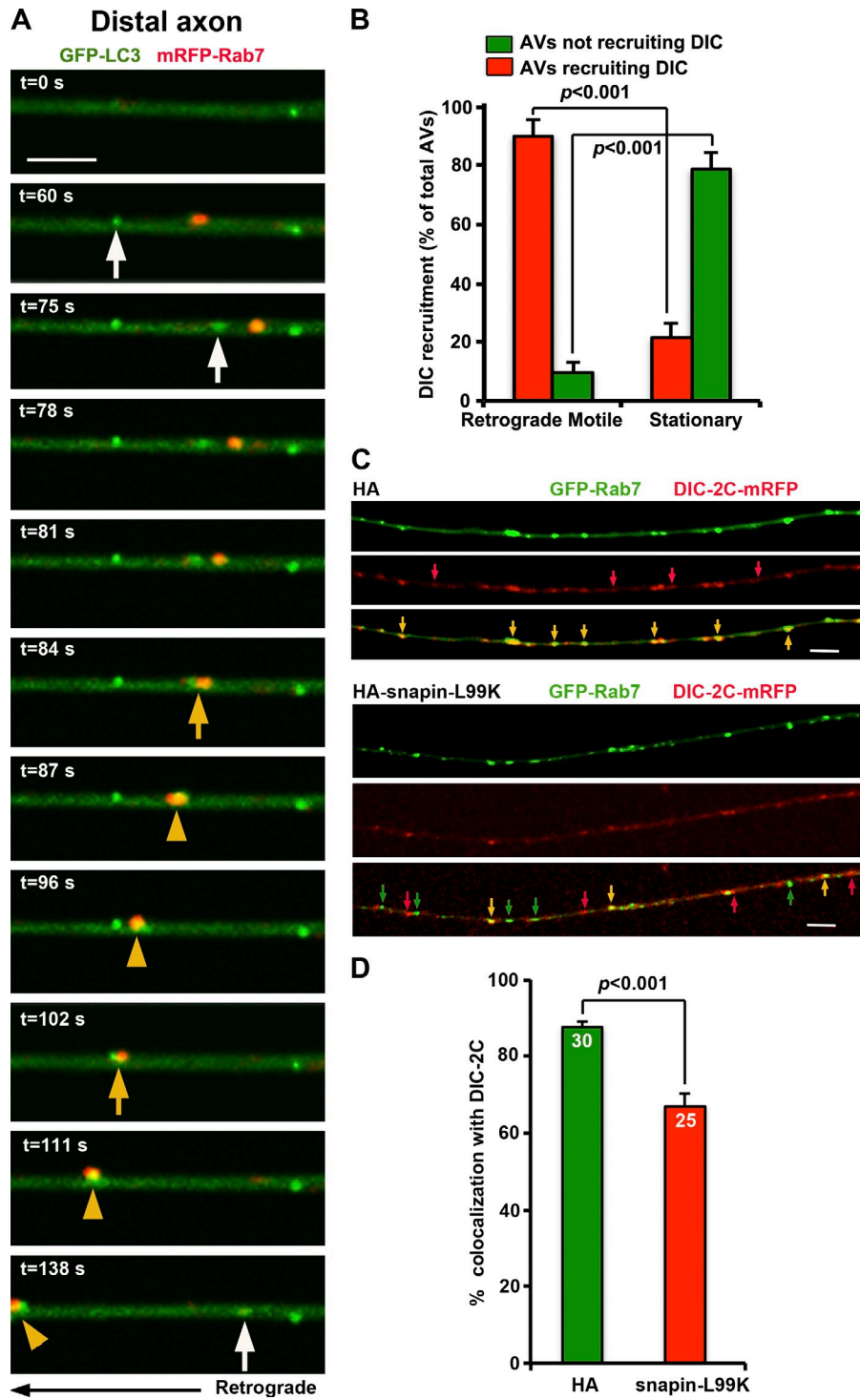
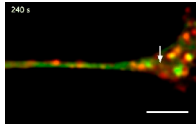


Figure S3. **Dynamic de novo autophagosomal biogenesis, fusion, and retrograde transport along the distal axon shaft of a DRG neuron.** (A) Time-lapse images were taken every 3 s with acquisition exposure time at 150 ms in a Nikon spinning-disk confocal A1R with the PFS (Apochromat 100 \times , 1.49 NA oil immersion objective) in an environmental chamber at 37 $^{\circ}$ C. White arrows point to the appearance of new autophagosome (green) in the distal axon shaft at 60, 75, and 138 s; yellow arrows denote the fusing of autophagosome with LE at 84 and 102 s; and yellow arrowheads indicate a retrograde motile amphisome toward the soma between 87 and 138 s after fusion occurred. (B) Quantitative analysis showing relative DIC-2C recruitment to stationary versus retrograde motile AVs (GFP-LC3) after expression of Stx17-siRNA or control Scr-siRNA in live DRG neurons ($n = 40$). Note that the majority (90.11%) of retrograde motile AVs recruit DIC-2C, whereas only a small portion (21.37%) of stationary AVs are labeled by DIC-2C. (C and D) Representative images and quantitative analysis showing that disrupting snapin-DIC coupling by overexpressing snapin-L99K reduces recruitment of DIC to LEs. Yellow arrows indicate LEs recruiting DIC-2C, green arrows indicate LEs not recruiting DIC-2C, and red arrows point to DIC-2C not associated with LEs. The total neuron numbers for quantification were indicated inside the bars. Bars, 5 μ m. Error bars: SEM. Mann-Whitney test.



Video 1. Dynamic de novo autophagosomal biogenesis, fusion, and retrograde transport in the growth cone of a DRG neuron. DRG neurons were cotransfected with autophagy marker GFP-LC3 (green) and LE marker mRFP-Rab7 (red) at DIV0 and imaged at DIV3 immediately after starvation. Time-lapse images were taken every 3 s with acquisition exposure time at 150 ms in a Nikon spinning-disk confocal. White arrow points to the appearance of a new autophagosome (green) within the growth cone, and the yellow arrow indicates fusion with a LE (red) into an amphisome (yellow) and moving away from the growth cone. The time for completing these three steps is ~ 1 min. Bar, 5 μm .